HEFAT2007
5th International Conference on Heat Transfer, Fluid Mechanics and Thermodynamics
Sun City, South Africa
Paper number: LD1

STUDY AND COMPARISON OF RESULTS OF EXPERIMENTAL AND NUMERICAL SOLUTIONS FOR HYDRAULIC ANALOGY

Lavicka D.*, Polansky J., Boiron O.
*Author for correspondence
New Technologies – Research Centre,
University of West Bohemia in Pilsen,
Pilsen, 2007,
Czech Republic,
E-Mail : dlavicka@ntc.zcu.cz

ABSTRACT

The hydraulic analogy existing between the propagation of wavelets at the free surface flow of a liquid and the propagation of acoustic waves in a compressible gas is used to study aerodynamics problems with phenomena at flow around solids at supersonic velocities and aeroacoustic phenomena in supersonic divergent jets. In particular, water level fluctuations, which are proportional to pressure fluctuations in the gas, are measured with an optical fiber and special measuring apparatus. Investigations are carried out on a convergent-divergent (de Laval) nozzle. This phenomenon is linked to the existence of shock-cells in supersonic jets, which are formed in the output of the nozzle. These experimental results will be compared with the results from numerical solution and will be obtained from our own program and from the commercial program CFD Fluent.

INTRODUCTION

The hydrodynamic analogy exists between three-dimensional free surface flow and two-dimensional inviscid compressible flow. The propagation of weak pressure pulses (sound waves) in a two-dimensional compressible flow can be considered as compared to the movement of small amplitude waves (wave speed) on the surface of free surface flow. Both flows are strikingly similar in several ways and in each case the influence of flow velocity on wave pattern is similar. In the first case, when the flow velocity is less than the wave speed, the flow is **subsonic** for compressible flow and **subcritical** for free surface flow. In the second case, when the velocity flow is equal to the wave speed, the flow is **sonic** for compressible flow and **critical** for free surface flow. In the third case, when the flow velocity is greater than the wave speed, the flow is **supersonic** for compressible flow and **supercritical** for free surface flow. Normal shocks can occur in supersonic compressible flow and similar phenomena can be viewed in supercritical free surface flow. Comparison of the characteristics at both flows suggests a strong resemblance and thus between the two phenomena.

Free surface flow is demonstrated with a shallow water level. Shallow water level is fluid flow, which has water depth of approximately 100 mm. Free surface flow is advantageous, because it is very inexpensive when compared to compressible flow. Its biggest advantages are low cost and low price of experimental equipment. This experiment has a simple

NOMENCLATURE

A	[m^2]	Area
B	[m]	Width
c	[m/s]	Velocity
c_p	[kJ/kgK]	Specific heat by constant pressure
D_w		Steadying term for matrix of our own programme
e		Internal energy
E_v	[N/m^2]	Bulk modulus of elasticity
F		Matrix of our own programme
Fr	[-]	Froude number
G	[m /s^2]	Acceleration of gravity
h	[m]	Depth of water level
H		Matrix of our own programme
Ma	[-]	Mach number
p	[Pa]	Pressure
R	[J/Kmol]	Constant of gas
$t\,(\tau)$	[s]	Time
T	[°C],[K]	Temperature
u	[m]	Vector axis direction
v	[K]	Vector axis direction
V	[m/s]	Velocity
W_k		Matrix of our own programme
w	[m]	Vector axis direction
x	[m]	Cartesian axis direction
y	[m]	Cartesian axis direction
z	[m]	Cartesian axis direction

Special characters

κ	[-]	Constant of gas
Ψ	[-]	Efficiency of leaving coefficient
π	[-]	Ludolph's number

Subscripts

c	Compressible flow
oc	Free surface flow
k	Step count of time
n	Step count of space

construction with which it is possible to carry out more experimental measuring. In these experimental measurements can be good visualization and illustration of individual phenomena, which are important for Hydrodynamic analogy. In this experiment can be measured models, which have a size approximately from 5 to 50 centimeters and can be modelled a complicated unsteady process.

Hydrodynamic analogy does not have only advantages, but also several disadvantages. One disadvantage is its limitation only for surface case. Hydrodynamic analogy isn't valid for three-dimensional flow at compressible flow. Numerical simulation and modelling can use only hypothetical gas. This gas isn't really gas, because κ for hypothetical gas is equal to 2. Efficient utilization would be in case we knew the rate of exchange for real gas, but this time the rate of exchange is unknown.

RELATIONS OF HYDRODYNAMIC ANALOGY

The basic idea consists of sinusoidal surfaces of waves of small amplitude propagation at water level of hydrodynamic analogy, which is moving at the speed according to the equation

$$c = \left[\frac{g\lambda}{2\pi}\tanh\left(\frac{2\pi y}{\lambda}\right)\right]^{1/2} \tag{1}$$

, where $tanh\left(\frac{2\pi y}{\lambda}\right)$ is the hyperbolic tangent of the argument $\frac{2\pi y}{\lambda}$.

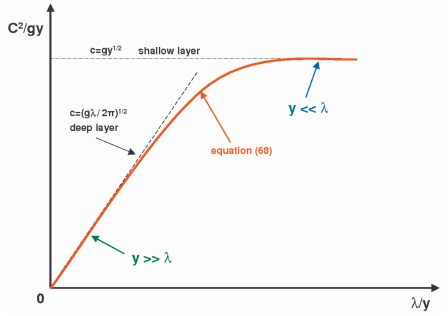

Figure 1 Wave speed as a function wavelength

Figure 1 shows two limiting cases for $tanh\left(\frac{2\pi y}{\lambda}\right)$. The first case is valid for conditions where depth is much greater than wavelength ($y >> \lambda \Rightarrow y/\lambda \to \infty$, for example ocean), the wave speed is independent of y and given by

$$c = \sqrt{\frac{g\lambda}{2\pi}} \tag{2}$$

The second case is valid if the fluid layer is shallow ($y << \lambda \Rightarrow \Rightarrow y/\lambda \to 0$) as often used in free surface flow, the wave speed is given by

$$c = (gy)^{1/2} \tag{3}$$

We can compare speed between velocity of surface propagation waves at water level and velocity of sound propagation waves (*the acoustic velocity or the speed of sound, c*). The speed of sound is related to changes in pressure and density of the fluid medium at isentropic process through the equation

$$c = \sqrt{\left(\frac{dp}{d\rho}\right)_s} = \sqrt{\left(\frac{E_v}{\rho}\right)_s} \tag{4}$$

, this expression was derived from the phenomena of acoustics [1], [4], [6], [9]. Speed of sound is larger in fluids that are more difficult to compress.

For our case will be used perfect (ideal) gas undergoing an isentropic process

$$c = \sqrt{\kappa RT} = \sqrt{\kappa\frac{p}{\rho}} \tag{5}$$

From comparison the speed wave propagation at the water level is less than wave speed. This low speed wave propagation at water level is the main advantage of hydrodynamic analogy for free surface flow.

In this section we begin to describe compressible flows by basic equations for two-dimensional flow. The forms of the basic equations in a two-dimensional compressible flow are discussed in the following paragraphs.

The continuity equation is valid for steady or unsteady flow, and compressible or incompressible fluids. In vectors the shape can be written as

$$\frac{\partial\rho}{\partial t} + \frac{\partial\rho u}{\partial x} + \frac{\partial\rho v}{\partial y} + \frac{\partial\rho w}{\partial z} = 0 \tag{6}$$

The next basic equations of Hydrodynamic analogy are Equations of Motion. We will suppose only gravitational acceleration, which is parallel to the axis y. Gravitational acceleration had reverse direction, as shown in Figure 2.

$$-\frac{1}{\rho}\frac{\partial p}{\partial x} = \frac{\partial u}{\partial t} + u\frac{\partial u}{\partial x} + v\frac{\partial u}{\partial y} + w\frac{\partial u}{\partial z} \tag{7}$$

$$g - \frac{1}{\rho}\frac{\partial p}{\partial y} = \frac{\partial v}{\partial t} + u\frac{\partial v}{\partial x} + v\frac{\partial v}{\partial y} + w\frac{\partial v}{\partial z} \tag{8}$$

$$-\frac{1}{\rho}\frac{\partial p}{\partial z} = \frac{\partial w}{\partial t} + u\frac{\partial w}{\partial x} + v\frac{\partial w}{\partial y} + w\frac{\partial w}{\partial z} \tag{9}$$

Equations (7), (8), (9) are the general differential equations of motion for the fluid in our case.

Consider a case where the waves propagate in the *x* direction only, and that the motion is two dimensional in the xy-plane (Figure 2). Direction *y* is measured upwards from the bottom surface, and *h* is the displacement of the free surface. The pressure at height *y* from the bottom, which is hydrostatic, is given by

$$\delta p = \rho g \delta h \tag{10}$$

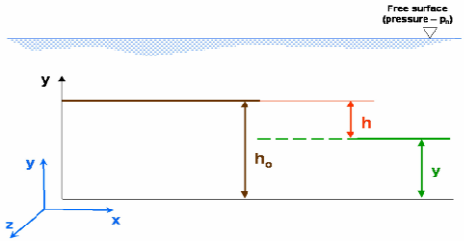

Figure 2 Notation for pressure variation in a fluid at rest with a free surface

In our case it is valid that load to fluid is only acceleration of gravity g. And substitution conditions according to Figure 2, where depth is, $h = h_o - y$ can be given as

$$p = p_o + \rho g h \tag{11}$$

The hydrodynamic analogy solves only surface case in the plane xy-plane. And then can be reduced from 3 equations of motion to 2 equations (12), (13).

$$-\frac{1}{\rho}\frac{\partial p}{\partial x} = \frac{\partial u}{\partial t} + u\frac{\partial u}{\partial x} + w\frac{\partial u}{\partial z} \tag{12}$$

$$-\frac{1}{\rho}\frac{\partial p}{\partial z} = \frac{\partial w}{\partial t} + u\frac{\partial w}{\partial x} + w\frac{\partial w}{\partial z} \tag{13}$$

The equation (10) substitutes to equations (12), (13), where the left side is modified from non-conservative form to conservative form and then we give final relations

$$-\frac{1}{h}\frac{\partial(\frac{1}{2}gh^2)}{\partial x} = \frac{\partial u}{\partial t} + u\frac{\partial u}{\partial x} + w\frac{\partial u}{\partial z} \tag{14}$$

$$-\frac{1}{h}\frac{\partial(\frac{1}{2}gh^2)}{\partial z} = \frac{\partial w}{\partial t} + u\frac{\partial w}{\partial x} + w\frac{\partial w}{\partial z} \tag{15}$$

Comparing equations (12), (13) and (14), (15) and the density is analogous to depth h.

The hydrodynamic analogy can be used only for isoentropic hypothetical air flow with nominal value of air $\kappa = 2$. These conditions and other relations can be used for deriving other values (for example density, velocity, specific heat ratio, etc.), which are mutually analogous. Analogue magnitudes between compressible flow and free surface flow are stated in Table 1.

	compressible flow	open-channel flow
Density ρ	ρ	*depth* h
Pressure	p	$\frac{gh^2}{2}$
Velocity	V	V_{oc}
Speed of sound *vs.* Wave speed	$c = \sqrt{\kappa RT}$	$c_{oc} = \sqrt{gy}$
Mach number Ma *vs.* Froude number Fr	$Ma = \frac{V}{c}$	$Fr = \frac{V_{oc}}{c_{oc}}$
Area *vs.* width	A	*width* b
Specific heat ratio	κ	2
Specific heat at constant pressure	c_p	g
Specific heat at constant volume	c_v	$g/2$

Table 1 Summary of analogue magnitudes between compressible flow and free surface flow

OUTLINE OF EXPERIMENT

This apparatus was built at "l'Ecole Centrale de Marseille"[Lávička, 2005], which is shown in Figure 1. and Figure 2. This experiment consisted of two reservoirs (Reservoir and Spillway), which are connected by a surface plane, the table analogy. Recirculation of water at table analogy is secured by the help of a pump. Water is pumped from the spillway and next goes through several valves, where water depth can be regulated in the reservoir and water depth can be regulated by means of a by-pass. Next it goes through the water filter and Venturi tube, where pressure of water can be measured and mass flow rate can be computed from this pressure of water. It goes through the Venturi tube. Pumped water supplies the reservoirs. Water flow from the reservoir through convergent-divergent nozzle and the circuit is repeated.

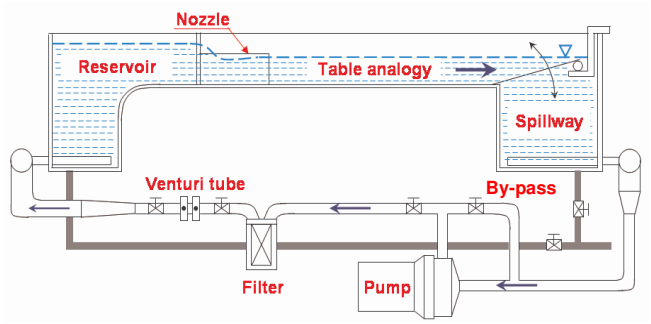

Figure 3 Scheme of experimental apparatus

The nozzle has convergent-divergent shape. It was produced from plastic material that is merged with the barrier. Nozzle and barrier can be exchanged with other shapes of nozzles.

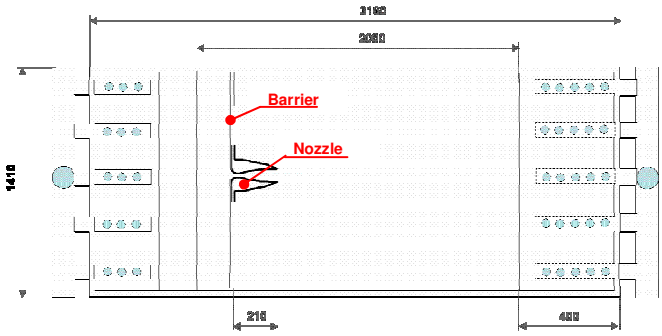

Figure 4 General sizes of experimental apparatus

This table analogy is created from a sheet of glass. The water-level fluctuations of the experimental apparatus can be observed through the glass. Water level depth on table analogy is regulated by several valves and by spillway (S) with water depth regulator (RH).

NUMERICAL METHOD

This part describes the numerical method, which solves the phenomena of hydrodynamic analogy by commercial software and our own program.

Our own program

Our own program [4,8] solves 1-dimensional compressible flow. This special code was written in the Matlab. It was created for better understanding of these phenomena. The special program has several advantages, for example faster computation, easier setting of various shapes of nozzle and boundary conditions. Fundamental equations were used for solution in our own program. Three equations are basic relations for 1D :

- continuity equation

$$\frac{\partial \rho A}{\partial t} + \frac{\partial \rho A u}{\partial x} = 0 \tag{17}$$

- motion equation

$$\frac{\partial \rho u}{\partial t} + \frac{\partial (\rho u^2 + p)A}{\partial x} = \frac{p dA}{dx} \tag{18}$$

- energy equation

$$\frac{\partial eA}{\partial t} + \frac{\partial (e+p)uA}{\partial x} = 0 \tag{19}$$

- computational formula Lax-Friedrich (20)

$$W_k^{n+1} = \frac{1\Delta t}{2\Delta x}(F_{k+1}^n - F_{k-1}^n) + \frac{\varepsilon}{2}(W_{k+1}^n - 2W_k^n + W_{k-1}^n) + \Delta t H \tag{20}$$

This Lax-Friedrich formula was used as steadying resistance in the zone, where normal shock-wave occurs. Shock wave is shown as a downturn by pressure line and the opposite for Mach number.

The second step will use the detailed and more accurate McCormack computational formula. This formula is more exactly in the zone, where normal shock-wave occurs.

$$W_k^{n+\frac{1}{2}} = W_k^n - \frac{\Delta t}{\Delta x}(F_{k+1}^n - F_k^n) + \Delta t H_k^n \tag{21}$$

$$\overline{W}_k^{n+1} = 12(W_k^n + W_k^{n-\frac{1}{2}} - \frac{\Delta t}{\Delta x}(F_k^{n+\frac{1}{2}} - F_{k-1}^{n+\frac{1}{2}}) + \Delta t H_k^{n+\frac{1}{2}} \tag{22}$$

$$\overline{W}_k^{n+1} = W_k^{n+1} + DW_k^n \tag{23}$$

The commercial numerical program is based on the system of Navier-Stokes equations for turbulent flow of compressible flow and free surface flow. The numerical simulation was carried out using the CFD program FLUENT 6.2.16. The numerical simulation is solved by the Runge-Kutta method in the form of finite volumes. Convergence is evaluated through the computation of residuals.

Commercial programme – compressible flow

A computation mesh was created in pre-processing software Gambit 2.2.30. A standard quadratic grid was used to mesh the numerical domain, giving approximately 40 000 cells. This computation mesh was created for 2 dimensional numerical models.

The numerical simulation was carried out using the commercial CFD program FLUENT 6.2.16. The state equation of the compressible gas is added to the equation set. The numerical model is solved as coupled explicit 2D solver.

Boundary conditions are shown on Figure 5. At the input was defined in the computational model as boundary condition pressure-inlet and for the output was defined boundary condition the pressure outlet. For axis of symmetry was used boundary condition symmetry. In condition pressure inlet was defined by the help of change of pressure ratio in input. Gauge total pressure was changed at intervals 50 Pa - 300 000 Pa.

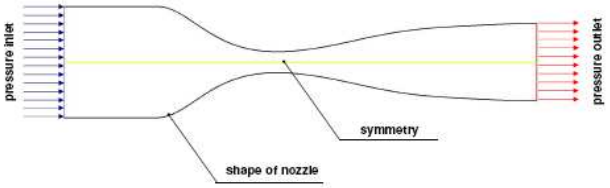

Figure 5 Boundary conditions for two-dimensional compressible flow

Commercial programme – free surface flow

A computation mesh was also created in software preprocessing Gambit 2.2.30. A standard hexahedron grid was used to mesh the numerical domain, giving approximately 500 000 cells.

As 3 dimensional it was numerical simulation of free surface flow with liquid water and air. The numerical simulation was carried out using the commercial CFD program FLUENT 6.1.22. The numerical model is solved as segregated 3D solver unsteady. It was set for free surface flow VOF (Volume Of Fluid Model) model. Boundary conditions are shown on Figure 6. At the input was defined in the computational model as boundary condition mass-flow-inlet and for the output was defined boundary condition the pressure-outlet. For axis of symmetry was used boundary condition symmetry. Other conditions were set as wall.

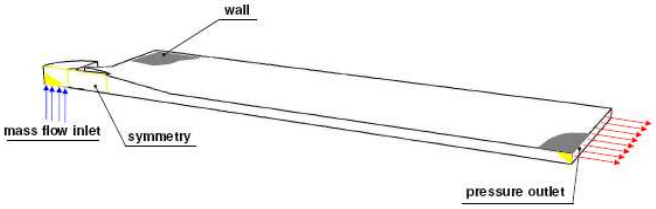

Figure 6 Boundary conditions for three-dimensional free surface flow

In condition mass-flow inlet two phases were defined. The first phase is air and second phase is water. In the conditions mass-flow rate was set at the size 0.55 kg/s. This quantity is half of mass-flow rate, because it was calculated only with half model. Summary mass flow rate 1.1 kg/s agrees with our experiment.

RESULTS

Experimental

Experimental apparatus was used for measuring various magnitudes and characteristics, which are important for hydrodynamic analogy. Basic laws of hydrodynamic analogy are obtained and verified from measuring.

In the first step the dependence between mass flow rate in convergent – divergent nozzle and water depth of reservoir was measured. Mass flow rate was obtained from pressure, which was measured by Venturi tube. The Venturi tube placement is showed in Figure 3. This pressure was measured by two tubes, where water depth above floor is measured. Mass flow rate was computed on the basis of relation of Venturi tube. Results are

shown in Figure 7. Dependence between water depth in the reservoir and mass flow rate was used for boundary conditions in the numerical simulations. Red points measure values and the blue line is the interpolating line.

The next measurement measured and verified the leaving coefficient (Ψ), which is given for existing material. The leaving coefficient depends on constant κ and ratio pressure (see equation 24 and 25 from [4], [9]).

$$m_\tau = S\sqrt{\frac{\kappa}{\kappa-1}[(\frac{p}{p_0})^{2/\kappa} - (\frac{p}{p_0})^{\kappa+1/\kappa}]}\sqrt{2\frac{p_0}{v_o}} \tag{24}$$

$$m_\tau = S\psi\sqrt{2\frac{p_0}{v_o}} \tag{25}$$

Values of leaving coefficient (Ψ) can be represented as dependence in the pressure ratio p/p_0 shown by the red curve (Figure 8) for κ = 1.4, this value is valid for standard air. The red curve shows only an illustrative example.

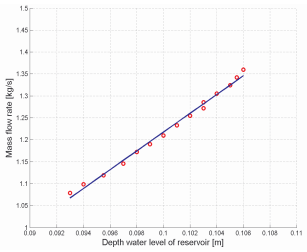

Figure 7 Dependence between depth of reservoir and mass flow rate

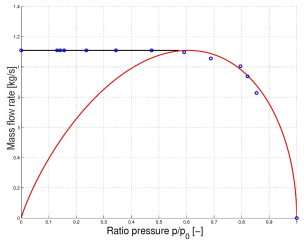

Figure 8 Real course of leaving coefficient

The last type of measurement was important, because this experimental measuring will be compared with other results of numerical solution from our own programme, two–dimensional compressible flow and three–dimensional free surface flow.

In Figure 9 is shown measuring apparatus, which is composed of several parts. Water depth was measured by micrometers, which are fixed to the saddle above water level. This measurement was taken in 21-steps (positions) along the axis of symmetry. Direction and measurement nozzle are shown in Figure 9.

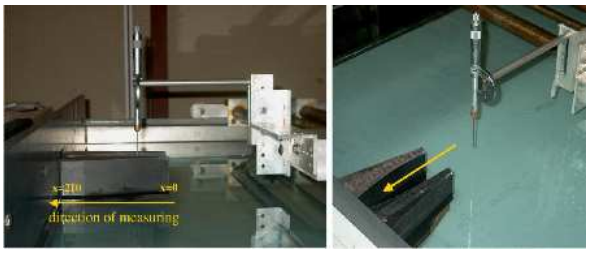

Figure 9 Measuring device

Regulation of water depth and mass flow rate was realized by pump with by-pass and valves. Following this, the water depth in the reservoir is changed. Furthermore, regulation of water depth in Table Analogy was provided. This change is important for simulating different states of flows through convergent–divergent nozzle. Subcritical, critical and supercritical flow can be obtained this way. Water depth in Table Analogy was changed by spillway at water depth intervals from 0 to 100 mm.

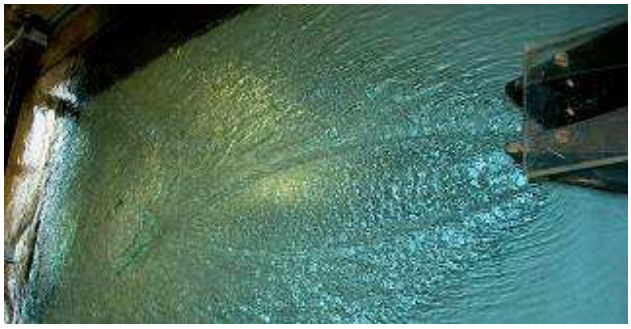

Figure 10 Water level at outlet from nozzle of experiment

Graphs (Figure 11) displayed normalization of water depth in individual measured points along axis of symmetry in convergent–divergent nozzle. Normalization of water depth is obtained as the rate between H/H_0, axis *y*. Axis *x* shows position in nozzle. This Figure shows course of water depth level for different types of free surface flows. Here is represented the behaviour of water level of nozzle subcritical flow (upper cyan curve) and for supercritical flows (other curves). Curves of supercritical flows have shock wave in convergent–divergent nozzle. For the last curve (lower blue curve), the shock wave is at the output of the nozzle. The shock wave can be seen in the Table analogy, where it is shown as a change in water depth level. Water depth in reservoir and spillway was recorded during measuring water depth in nozzle.

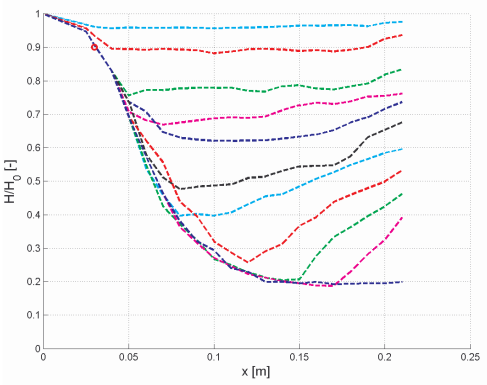

Figure 11 Course of water depth in nozzle

NUMERICAL PROGRAMS

Outputs from our own program are matrix magnitudes, which are described in the previous chapter Numerical method. These outputs can be shown most often as graphs with course of pressure and Mach number along convergent–divergent nozzle. Results from our own program are processed in graphs, which compare individual results from numerical method (Figure 14 and 15). Next, numerical method is solved by commercial program Fluent 6.2.16. This program makes it possible to investigate more magnitudes compared to our own programme. In Figure 12 is shown graphical results of Mach number for 2-dimensional compressible flow for pressure ratio

p/p0=0.985 (subsonic flow) and pressure ratio p/p0=0.503 (supersonic flow)

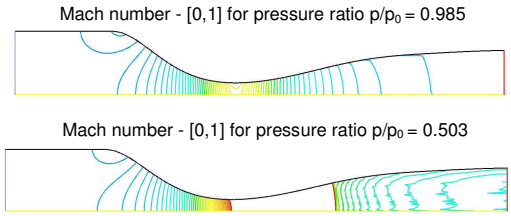

Figure 12 Graphical results from 2-dimensional flow

In the case where subsonic flow Mach number is less than 1 in minimal cross-section of nozzle then a shock wave does not occur. This case is shown at left in Figure 12. The opposite situation is at right in Figure 12. Here a shock wave occurs in minimal cross-section of nozzle and its length is dependent on the size of the Mach number. The shock wave is shown in Figure 12 as "white" area of nozzle for Mach number.

Three-dimensional flows have the biggest demands on numerical solution, which simulate free surface flow. The biggest demands relate to computational time and size of computational mesh. This case shows course of water level along convergent-divergent nozzle. Figure 13 shows the case for supercritical flows of the nozzle.

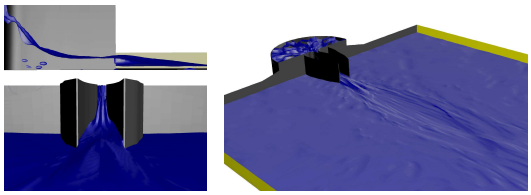

Figure 13 Course of water level from 3-dimensional flow

Now results can be compared from numerical methods (our own program, compressible flow and free surface flow) and measured experimental values.

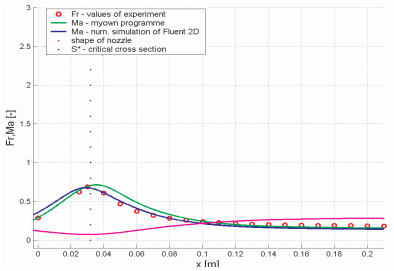

Figure 14 Comparison results for subsonic and subcritical flows

These results are described in Figure 14 and 15. Figure 14 shows the course of subsonic flow and Figure 15 is for subcritical case. Values of Mach number for compressible 2D flow and Froude number for 3D free surface flow are compared in the Figures.

CONCLUSION

In this article, we compared results obtained by fluid flow numerical simulations and experimentally. The fluid flow simulations were computed for compressible flow and free surface flow by several methods. These numerical results for subsonic and subcritical flow are in agreement with the experimental results. But for supersonic and supercritical we

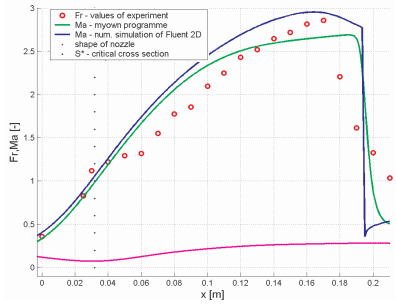

Figure 15 Comparison results for supersonic and supercritical flow

observe small differences in the sphere higher Mach's number and Froude's number. The variation is caused by the roughness set-up of nozzle material and glass, which creates table analogy.

The next step will be to incorporate in the numerical simulation our own program, by using different computational formula as for example McCormack. Our own program can be used for different shapes nozzle in the case for compressible flow, because its main advantage is that the computational time is shorter than with Fluent 6.2.16.

ACKNOWLEDGEMENT

This paper is based upon cooperation between the University of West Bohemia in Pilsen and l'Ecole Centrale de Marseille – laboratory in Marseille. This paper is based upon work sponsored by the Ministry of Education of the Czech Republic under research and development project 1M06031.

REFERENCES

[1] Lavicka, D.: *The study analogy between compressible flow and free surface flow (experiments and diagnostics)*, EGIM laboratory, Marseille, France, 2005.

[2] Lavicka, D.; Boiron O; Polansky J.: *Simulation CFD d'une analogie entre un ecoulement compressible et un ecoulement á surface libre,* Fluent Forum 2007, Paris, France, 2007.

[3] Lavicka, D; Boiron, O..;: *"CFD simulation of analogy between compressible and free surface flow"*. 3rd International PhD Conference on Mechanical Engineering – PhD 2005, str. 105-106, Srni, ČR, 2005. ISBN 80-7043-414-7.

[4] Munson, B.,R.; Young, D., F.; H. Okiishi, T., H.: *"Fundamental of Fluid Mechanics"*. Third edition. Oiwa State, University, Ames, Iowa, USA, 1998.

[5] Fluent 6 "User's Guide", 2002.

[6] Makhsud, A.;: These – *"Étude expérimentalé de L'instabilité et de L´émission acoustique de jets supersoniques sous-détendus*" (Simulation en Analogie Hydraulique), Marseille, France, 1996.

[8] Kozel K.; Furst J. : *Numericke metody reseni problemu proudeni I*, 1. vydani, vydavatelstvi CVUT, Praha, 2001.

[9] Kalcik J.; Sykora K.: *Technicka termomechanika*, 1. vydani, Academia, nakladatelstvi Ceske akademie ved, Brno, CR, 1973. ISBN 104-21-825.

[10] Carbonaro M.; Haegen V. V. : *Hydraulic analogy of supersonic flow – lab notes*. In EUROAVIA symposium, November 2002, Von Karman Institute for Fluid Dynamics.